© 2019. Published by The Company of Biologists Ltd | Journal of Experimental Biology (2019) 222, jeb189357. doi:10.1242/jeb.189357

RESEARCH ARTICLE

Thoracic adaptations for ventilation during locomotion in humans and other mammals

W. Éamon Callison*, Nicholas B. Holowka and Daniel E. Lieberman

ABSTRACT

Bipedal humans, like canids and some other cursorial mammals, are thought to have been selected for endurance running, which requires the ability to sustain aerobic metabolism over long distances by inspiring large volumes of air for prolonged periods of time. Here, we tested the general hypothesis that humans and other mammals selected for vigorous endurance activities evolved derived thoracic features to increase ventilatory capacity. To do so, we investigated whether humans and dogs rely on thoracic motion to increase tidal volume during running to a greater extent than goats, a species that was not selected for endurance locomotion. We found that while all three species use diaphragmatic breathing to increase tidal volume with increasing oxygen demand, humans also use both dorsoventral and mediolateral expansion of the thorax. Dogs use increased dorsoventral expansion of the thorax, representing an intermediate between humans and goats. 3D analyses of joint morphology of 10 species across four mammalian orders also showed that endurance-adapted cursorial species independently evolved more concavo-convex costovertebral joint morphologies that allow for increased rib mobility for thoracic expansion. Evidence for similarly derived concavo-convex costovertebral joints in *Homo erectus* corresponds with other evidence for the evolution of endurance running in the genus *Homo*.

KEY WORDS: Respiration, Thorax, Human evolution, Ribcage, Bipedalism, Endurance running

INTRODUCTION

Humans differ from other non-human primates, including chimpanzees, in being adapted more for endurance than for power and speed (Carrier et al., 1984; Bramble and Lieberman, 2004; O'Neill et al., 2017; Pontzer, 2017). Like other primates, chimpanzees rarely sprint and do so only for short distances of less than 100 m, followed by resting and intense panting (Hunt, 1991; Bramble and Lieberman, 2004). In contrast, humans are capable of sustained endurance activities such as trekking and endurance running, defined as running long distances (>5 km) over extended time periods using aerobic metabolism (Bramble and Lieberman, 2004). In humans, endurance running requires breathing as much as 1.3–2.5 l min^{-1} kg^{-1} (mass-specific minute ventilation; Weibel, 1984; Bulbulian et al., 1986). Only a few other running-adapted (cursorial) mammals, including dogs, wolves, camels and horses, are known to be capable of such sustained aerobic capacity (Coombs, 1978; Garland, 1983; Carrano, 1999). Among these species' adaptations for endurance running are increased maximal oxygen intake ($\dot{V}_{O_2,max}$) and respiratory capacity (Taylor et al., 1980; Seeherman et al., 1981; Gehr et al., 1981; Hildebrand, 1988; Bramble, 1989; Lindstedt et al., 1991; Poole and Erickson, 2011), and the ability to increase the volume of air inspired per breath (tidal volume; V_T) and per minute (minute ventilation, $\dot{V}_E$; Berry et al., 1996; Poole and Erickson, 2011) while changing the pattern of ventilatory and locomotory coordination (Bramble and Carrier, 1983; Bramble, 1989; Carrier, 1996; Boggs, 2002; Daley et al., 2013).

The human lung can meet the demands of aerobically intense exercise by increasing V_T up to 10-fold (Dempsey, 1985). However, the thoraco-abdominal elongation used by quadrupeds to increase V_T during locomotion (Marlin et al., 2002) may be physically constrained in humans by the arrangement of the viscera and the position of the thoracic cavity above the abdominal viscera due to upright bipedality. It is unknown whether the uniquely shaped human thorax contributes to its respiratory capabilities. Most research concerning the evolution of hominin thoracic morphology has focused on the transition from funnel- to barrel-shaped chests. Reconstructions indicate that fossils of *Australopithecus afarensis* (AL-288-1) and *Australopithecus sediba* (MH1 and MH2) have generally ape-like funnel-shaped thoraxes (although the upper thorax of one partial skeleton of *Au. afarensis*, KSD-VP-1/1, has been argued to be barrel shaped; Haile-Selassie et al., 2010). In contrast, fossils in the genus *Homo*, including *Homo erectus* (KNM-WT15000) and *Homo neanderthalensis*, typically have more barrel-shaped or bell-shaped thoraxes (Schmid, 1983; Trinkaus, 1983; Jellema et al., 1993; Franciscus and Churchill, 2002; Sawyer and Maley, 2005; Gómez-Olivencia et al., 2009; Haile-Selassie et al., 2010; Schmid et al., 2013; García-Martínez et al., 2014; Latimer et al., 2016; Bastir et al., 2017), though the preserved elements of *Homo naledi* suggest a narrow upper thorax and wide lower thorax (Williams et al., 2017).

Here, we tested the general hypothesis that humans, like other mammals apparently selected for vigorous endurance activities such as long-distance running, evolved derived thoracic features to increase ventilatory capacity. Normal, quiet inspiration in humans results almost entirely from intrathoracic volume changes caused by the contraction and flattening of the diaphragm (Weibel, 1984). In addition to diaphragmatic contraction, two main integrated types of movement permit the ribs to expand thoracic cavity size: the pump-handle (PH) and bucket-handle (BH) motions (Fig. 1). In the PH motion, the upper ribs pivot around their vertebral articulations, elevating their anterior ends and the attached sternum, expanding the thorax dorsoventrally. In contrast, the BH motion expands the thorax in the coronal plane by swinging the ribs that are attached to the body of the sternum (in humans, ribs 2–7) laterally and rotating them around both their vertebral and sternal articulations. As the ribs move cranially and caudally with both types of movement, the mediolateral and dorsoventral diameters of the rib cage change. PH

Department of Human Evolutionary Biology, Harvard University, 11 Divinity Avenue, Cambridge, MA 02138, USA.

*Author for correspondence (wcallison@g.harvard.edu)

W.É.C., 0000-0002-9467-8394; N.B.H., 0000-0003-0593-7524; D.E.L., 0000-0002-6194-9127

Received 25 July 2018; Accepted 1 October 2019

Journal of Experimental Biology (2019) 222, jeb189357. doi:10.1242/jeb.189357

List of symbols and abbreviations

BH	bucket handle
f_H	heart rate
$f_{H,max}$	maximum heart rate
f_R	respiration rate (breaths min^{-1})
IAF	inferior articular facet
ICF	inferior costal facet
M_B	body mass
PH	pump handle
SAF	superior articular facet
SCF	superior costal facet
$\dot{V}_E$	minute ventilation
$\dot{V}_{O_2,max}$	maximum amount of oxygen that an individual can utilize during maximal exercise
V_T	tidal volume
XROMM	X-ray reconstruction of moving morphology

and BH motions, and the resulting dorsoventral and mediolateral expansions, have been documented in immobilized, anesthetized dogs and cats during forced ventilation (Da Silva et al., 1977; Margulies et al., 1989), humans (Jordanoglou, 1970; Wilson et al., 1987; Saumarez, 1986), crocodylians (Brocklehurst et al., 2017) and squamates (Brainerd et al., 2016). Changes in thoracic dimensions have also been measured in running horses (Colborne et al., 2006; Thorpe et al., 2009).

Because it is difficult to measure how thorax shape might affect respiration in large numbers of species, we also explored here an alternative source of information, the morphology of the costovertebral joints. Costovertebral joint morphology has been assumed to reflect rib motion during locomotion in mammals because PH and BH rib movements originate at these joints. Joint surface curvature could provide an indication of overall joint mobility, with more curved joint surfaces theoretically indicating greater ranges of rib motion that might allow for increased dorsoventral and mediolateral thoracic expansion (Hamrick, 1996), but this has never been tested. Here, we determined whether concavo-convex joint morphology is present in animals known to increase thoracic volume through dorsoventral and/or mediolateral thoracic expansion and in animals known to engage in endurance behavior. If increased concavo-convex joints are observed, we can make predictions about potential thoracic motion in animals that we have not measured experimentally, including fossil species. Increased joint surface curvature is associated with increased mobility in many joints, but analyses of costovertebral joint structure in iguanas and alligators illustrate the difficulties of reconstructing rib movement based on joint morphology alone (Brainerd et al., 2016; Brocklehurst et al., 2017). In addition, intercostal function changes between ventilation and locomotion in lizards (Carrier, 1991) and birds (Codd et al., 2005; Tickle et al., 2007). Furthermore, variations in intercostal muscle function in dogs suggest that rib motion and thoracic function might change depending on locomotor behavior (Carrier, 1996), and that rib motion is different ipsilateral and contralateral to the forelimb of support during trotting (Bramble and Jenkins, 1993).

Here, to test whether costovertebral joint shape in the thorax of humans and other endurance-adapted cursorial species facilitates dorsoventral and mediolateral thoracic expansions that increase ventilatory capacity, we integrated experimental and comparative data to test four hypotheses. First, humans are predicted to supplement diaphragmatic respiration with dorsoventral and mediolateral thoracic expansions to increase overall volumetric expansion of the thoracic cavity during aerobically challenging activities in order to overcome constraints on ventilation due to bipedality. Second, dogs, which are an endurance-adapted cursorial animal, are predicted to supplement diaphragmatic breathing with thoracic movements, but primarily with dorsoventral rather than mediolateral thoracic expansion. Dogs are predicted to rely more on dorsoventral expansion because, like most cursorial quadrupeds, they have deep and narrow rib cages (resulting from flattened ribs

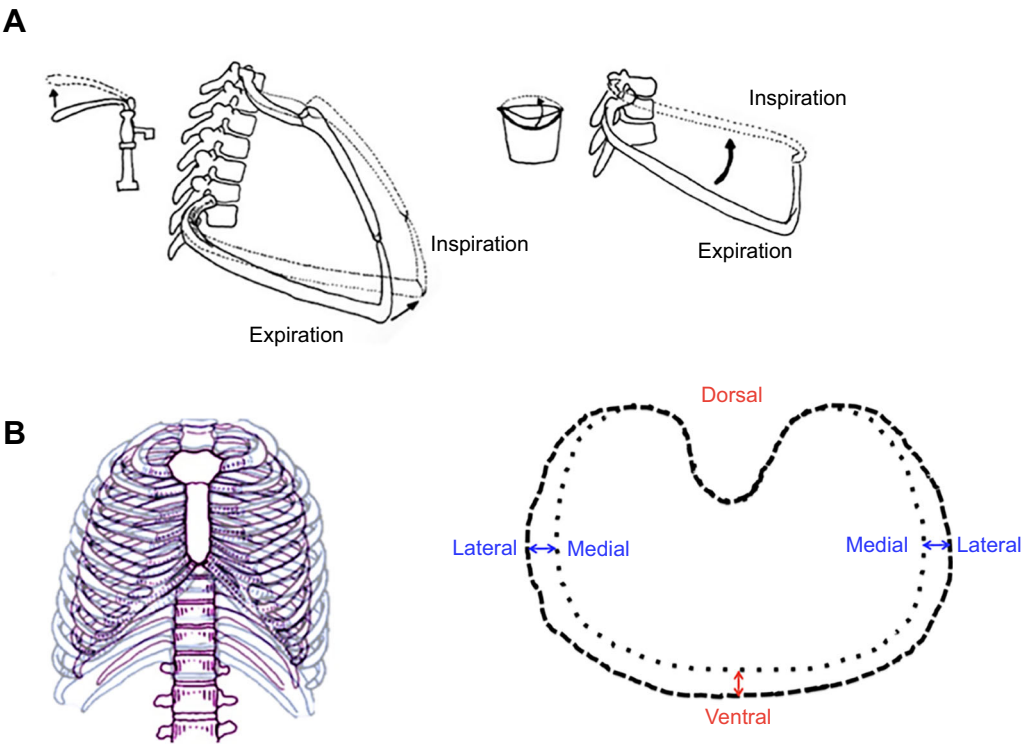

Fig. 1. Pump-handle (PH) and bucket-handle (BH) rib motions. (A) Left: dorsoventral thoracic expansion via PH rib motion. Right: mediolateral thoracic expansion via BH rib motion. Adapted from Aiello and Dean (1990). (B) Changes in the maximum circumference of the thorax during respiration due to pump-handle (dorsoventral; red) and bucket-handle (mediolateral; blue) motions in humans. The shape of the thorax during inspiration is represented by dashed lines and expiration is represented by dotted lines.

Journal of Experimental Biology (2019) 222, jeb189357. doi:10.1242/jeb.189357

with reduced lateral curvature and rib angles) that physically limit mediolateral thoracic expansion (Bramble, 1989). Furthermore, dogs are predicted to rely more on dorsoventral expansion because they must use their forelimbs to support their body weight via a thoracic muscular sling that attaches the scapula directly to the thorax (Carrier et al., 2006), meaning mediolateral thoracic expansion could move the forelimbs in a way that might de-stabilize the forelimb joints during locomotion. Third, animals that employ more dorsoventral and/or mediolateral thoracic expansions to augment V_T are hypothesized to have more rounded costovertebral joint facets in which one articular surface is convex while its corresponding surface is concave, allowing for greater rotation around the ribs' long axes and more flexion for increased BH and PH rib movements (Fig. 1). Finally, if this is true, we hypothesize that species known to engage in endurance running will have more curved joint surfaces than those that do not.

MATERIALS AND METHODS

Assessment of thoracic function

Subjects

Thoracic movement and respiration were measured in three species: humans, goats and dogs. For humans, 10 healthy, adult males with no history of major neuromuscular, cardiovascular or respiratory disease were recruited. Only male participants with BMI <25 were used to facilitate placement of surface markers directly on the skin of the thorax with minimal extraneous skin movement. All participants provided written informed consent, and prior approval for the experiments was obtained from the Committee on the Use of Human Subjects, Harvard University.

To compare humans with quadrupeds, three female Nubian goats (*Capra hiricus* Linnaeus 1758) and three (2 males and 1 female) greyhound dogs (*Canis familiaris* Linnaeus 1758) were also measured. Whereas dogs are endurance-adapted cursorial species, goats do not run long distances, have lower $\dot{V}_{O_2,max}$ relative to body mass than similarly sized cursors (Taylor et al., 1980), and are not considered very cursorial (Carrano, 1999). Harvard University Institutional Animal Care and Use Committee approval was obtained for the study, and institutional animal care guidelines were followed throughout.

Kinematics/experimental trials

All running was measured on treadmills. Human participants ran on an instrumented Bertec treadmill (Bertec, Columbus, OH, USA); dogs and goats ran on a custom-built treadmill (Kram, 1989). All subjects wore heart rate (f_H) monitors (Polar, New York, NY, USA) placed around the chest, cranial to the xiphoid process. To facilitate cross-species comparisons and to measure a range of exercise intensities, human participants completed a series of trials on the treadmill at rest and running at approximately 40%, 60%, 80% and 100% of maximum heart rate ($f_{H,max}$). $f_{H,max}$ in humans was measured by having participants run on a treadmill at increasing speeds and inclines until f_H plateaued at maximum effort.

$\dot{V}_{O_2}$ and associated f_H were measured in dogs and goats using a PA-10 oxygen analyzer (Sable Systems, North Las Vegas, NV, USA) while they were trotting at the fastest speeds they would sustain (2.0–2.23 m s^{-1} for goats; 2.8–3.0 m s^{-1} for dogs). Estimated $f_{H,max}$ values (Table S1) were calculated based on these measurements and previously measured $\dot{V}_{O_2,max}$ values for dogs (Lucas et al., 1980) and for goats (Taylor et al., 1980):

$$\text{Estimated } f_{H,max} = \frac{f_{H,measured} \times \dot{V}_{O_2,max}}{\dot{V}_{O_2,measured}}. \quad (1)$$

Dogs also completed a similar series of trials on the treadmill at rest and while running at heart rates that ranged between 35% and 50% of estimated $f_{H,max}$. Goats completed a similar series of trials on the treadmill at rest and while running at heart rates that ranged between 60% and 100% of $f_{H,max}$. When measuring thoracic motion, human speeds ranged from 1.3 to 5.1 m s^{-1}, goat speeds ranged from 1.5 to 2.23 m s^{-1} (trotting) and dog speeds ranged from 1.25 to 3.0 m s^{-1} (trotting). Inspiratory flow and volume were measured using a spirometer (ML311, ADInstruments, Colorado Springs, CO, USA) attached to a one-way flow respirometry mask with outputs recorded using Lab Chart spirometry software (ADInstruments). We measured respiration rate (f_R) and V_T at increasing f_H (Table S1).

To record thoracic movements in humans, 26 reflective markers were applied to the thorax (Fig. 2). Five markers, evenly spaced between C7 and T12, were used to define the spine. An additional six markers were used to define the dorsal portion of the thorax, arranged in three evenly spaced rows from the thoracic inlet to the lower costal margin. Nine markers were similarly placed on the ventral thorax, with three used to distinguish the sternum, from the manubrium to the xiphoid process. Three markers were placed under both arms on the lateral aspects of the thorax.

Because of differences in shape and size, the thoraxes of goats and dogs were covered with 16 markers and 18 markers, respectively (Fig. 2). In these species, three evenly spaced markers were used to define the spine, and three evenly spaced markers were used to distinguish the sternum from the manubrium to the xiphoid process. In goats, five markers in two evenly spaced rows placed on both sides defined the lateral aspects of the thorax from the thoracic inlet to the lower costal margin. In dogs, six

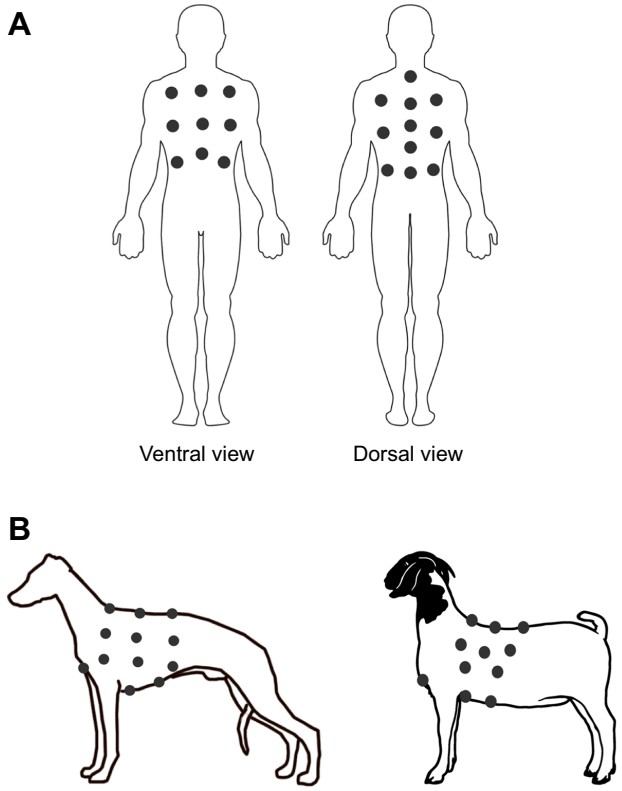

Fig. 2. Marker placement. (A) Approximate reflective marker placement on human participants (ventral and dorsal views). (B) Approximate reflective marker placement on dog and goat subjects (sagittal view).

Journal of Experimental Biology (2019) 222, jeb189357. doi:10.1242/jeb.189357

markers in two rows of three defined the lateral aspects of the thorax. In order to reduce surface marker errors due to extraneous movement of hair and skin, goats had small portions of their thorax shaved to facilitate marker placement. Lean, shorthaired greyhounds were used as canine subjects to reduce possible marker error from hair and skin movement. Furthermore, markers were placed on thoracic regions lacking substantial subcutaneous soft tissue and away from forelimb musculature.

Marker data were captured at 200 Hz using eight infrared Oqus cameras (Qualisys Corp, Gothenburg, Sweden) positioned around the treadmill. Marker data were cleaned in Qualisys Track Manager (Qualisys Corp) and processed in a custom-written MATLAB (MathWorks, Natick, MA, USA) program (written by W.É.C.) to calculate the volume of the thorax with respect to time. The program creates a 3D representation of the thorax in Euclidean space by connecting each point to every other measured point, using a triangular convex hull to generate a 3D shape from these points, and calculates the volume contained within the maximum 3D shape (orthogonal fit ratio=0.999; see 'Statistical analysis', below). Thorax volume was calculated from each frame over the course of 10 complete breaths per experimental condition. Maximum dorsoventral thoracic expansion was measured as the maximum change in distance between the most protruding pair of markers on the sternum and spine; maximum mediolateral thoracic expansion was measured using the most protruding pair of markers on the lateral aspects of the thorax. From these measurements, PH and BH rib motions were inferred.

Statistical analysis

Data analysis was performed in JMP Pro 13 (SAS Institute Inc., Cary, NC, USA) and R (http://www.R-project.org/). Because mammalian lung volume scales isometrically with body mass (Gehr et al., 1981), V_T was standardized by each subject's body mass. Likewise, maximum dorsoventral and mediolateral thoracic expansion was standardized by subject chest depth and width (average chest depth and width during the trial), respectively. Changes in thoracic volume were measured as the difference in thoracic volume between inspiration and expiration. The change in thoracic volume per breath was then standardized to the average volume of the thorax for each trial and calculated as the percentage change to allow cross-species comparisons.

To account for repeated measures and non-parametric data, non-linear mixed effects models using generalized least squares were used to assess fixed effects on thoracic response variables across species. Individual subject ID was included as a random effect and subjects were treated as a random sample from larger populations. Differences in slope between groups were assessed using a repeated measures ANCOVA. Differences in resting thoracic volume change were assessed using a pairwise Tukey's HSD.

Finally, to assess the reliability and accuracy of our volumetric calculations of thoracic volume, we used the above methods to measure the volume of a standard cylinder of known volume. Our volumetric assessment method was then tested using an orthogonal regression test examining the linear relationship between two continuous variables and comparing expected volume measurements with those observed/measured.

Measurements of costovertebral joint morphology

Measurements were taken from skeletons with complete or near-complete rib cages and vertebral columns from the following species: *Homo sapiens* (*N*=7; 3 adult males, 1 sub-adult male and 3 adult females), *Pan troglodytes* (*N*=7; 2 adult males, 2 adult females, 2 adults of unknown sex and 1 juvenile of unknown sex), *Capra hiricus* (*N*=3; adult females), *Canis familiaris* (*N*=2; adults of unknown sex), *Canis lupus* (*N*=2; 1 adult female, 1 adult of unknown sex), *Ursus americanus* (*N*=3; 1 male adult, 1 female adult and 1 adult of unknown sex), *Equus caballus* (*N*=3; adults of unknown sex), *Camelus dromedarius* (*N*=2; 1 male adult and 1 adult of unknown sex), *Rhinoceros unicornis* (*N*=1; 1 adult of unknown sex), *Dicerorhinus sumatrensis* (*N*=1; 1 adult of unknown sex) and *Merycoidodon culbertsoni* (*N*=2; 2 specimens of unknown sex and age). 3D images were also collected from research casts of the four hominin species with well-preserved thoraxes: *Au. afarensis* (AL-288), *Au. sediba* (MH1 and MH2), *H. erectus* (KNM-WT15000) and *H. neanderthalensis* (Shanidar 2, Shanidar 3 and Dederiyeh 2). Modern human, *Australopithecus* and *H. erectus* specimens were selected from the Peabody Museum of Archaeology and Ethnology (Cambridge, MA, USA), quadrupedal specimens from the Museum of Comparative Zoology at Harvard University, and Neanderthal specimens from the National Museum of Natural History (Washington, DC, USA). Ribs 4–7, as well as corresponding vertebrae, were identified on the basis of length, increasing inferior angle and changes in twist of the superior external border following Dudar (1993) and based on notations made during specimen collection and preparation.

The superior and inferior articular facets of ribs 4–7, the inferior and transverse costal facets on thoracic vertebra 3, and the superior, inferior and transverse costal facets on thoracic vertebrae 4–7 were measured. For each joint, a minimum of 40 photographic images of the ribs' superior and inferior articular facets, as well as a minimum of 60 images of the corresponding superior and inferior costal facets on the corresponding vertebrae, were taken using a Casio EX-XZR100 (resolution: 4000×3000 pixels). Images for each joint were compiled using a photometry program (PhotoScan, Agisoft, St Petersburg, Russia) to build 3D *in silico* models of the skeletal elements. The models were composed of fine mesh grids containing a minimum of 200,000 faces. The mesh grid faces corresponding to each portion of the costovertebral joint were manually selected to define the contours of the entire joint surfaces in the cranial–caudal plane, and the curvature of each articular facet was then measured using Geomajic software (Geomajic Control, 3D Systems, Rock Hill, SC, USA) by fitting a cylinder to the selected region. For each costovertebral joint facet, Geomajic was also used to measure the radius of curvature as the radius of a cylinder of best fit applied to the entire joint surface, and to calculate the included angle using the measured radius of curvature and measured length of the secant produced at the points where the cylinder of best fit and surface first come into contact. Convex facets were denoted as positive, while concave facets were denoted as negative. Increasing angle value indicates increasing concavo-convexity of the facet. Facets with no curvature in the cranial–caudal plane were designated to have an included angle of 0. The included angle measurement was repeated 5 times for each element to assess repeatability, and the average was used for data analysis. To test for reliability and accuracy, this method was performed on a cylindrical object of known curvature (orthogonal fit ratio=0.999).

Statistical analysis

Statistical analysis was performed in JMP Pro 13. To account for repeated measures, a generalized linear mixed model was used to assess the effect of genus and facet type (fixed effects) on costovertebral joint concavo-convexity, as well as the similarity between vertebral and corresponding rib joint facets. Repeated

Journal of Experimental Biology (2019) 222, jeb189357. doi:10.1242/jeb.189357

included angle measurements were included as a random effect and specimens were treated as a random sample from larger populations. Comparisons for species pairs were assessed with a Tukey's HSD. Cohen's *d* effect size was used to determine significant differences in included angle of costovertebral joint elements. Following Barrentine (1991), a gauge repeatability test was used to assess the repeatability of individual measurements, with less than 10% measurement variation being rated as 'excellent' (Table S2). Despite the potential for error due to the circular nature of angular measurements, we found that linear methods were appropriate to analyze the joint facet data because of the nature of our data (Fig. S1).

RESULTS

Assessment of ventilation and thoracic function

Dorsoventral and mediolateral thoracic expansion differed between all three species (humans, goats and dogs). Maximum dorsoventral expansion increased with mass-specific V_T strongly in humans (slope±*S.* 2.17±0.19, 95% confidence interval, CI [1.80, 2.54], R^2=0.71) and relatively moderately in dogs (0.87±0.12, 95% CI [0.63, 1.11], R^2=0.79) at different rates (P<0.0001; Fig. 3). In contrast, maximum dorsoventral expansion decreased with increasing V_T (l kg^{-1}) in goats (−0.78±0.01, 95% CI [−1.64, 0.07], R^2=0.24), differing significantly from humans (P<0.0001) and from dogs (P=0.0004). Maximum mediolateral expansion increased with V_T (l kg^{-1}) in humans (1.30±0.12, 95% CI [1.07, 1.53], R^2=0.69; Fig. 3). Maximum mediolateral expansion decreased slightly in dogs with V_T (l kg^{-1}) (−0.07± 0.32, 95% CI [−0.71, 0.56], R^2=0.0; P=0.0001). Maximum mediolateral expansion also decreased in goats with V_T (l kg^{-1}) (−0.77±0.62, 95% CI [−1.98, 0.45], R^2=0.13), differing significantly from humans (P=0.0016), but not dogs (P=0.3255; Fig. 3). Comparisons of maximum dorsoventral thoracic expansion relative to chest depth at maximum V_T (l kg^{-1}) demonstrated significant differences between dogs and humans (mean±s.e.m. 0.079±0.007, 95% CI [0.063, 0.094]) and goats (0.001±0.015, 95% CI [−0.031, 0.033]; P=0.0003), and between humans (0.091±0.006, 95% CI [0.078, 0.104]) and dogs and goats (0.020±0.008, 95% CI [0.003, 0.036]; P<0.0001). Additionally, maximum mediolateral thoracic expansion relative to chest width at maximum V_T (l kg^{-1}) differed significantly between humans and dogs (0.051±0.004, 95% CI [0.043, 0.060]) and goats (0.002±0.008, 95% CI [−0.016, 0.020]; P=0.0001), and between humans (0.056±0.005, 95% CI [0.046, 0.067]) and dogs and goats (0.018±0.006, 95% CI [0.005, 0.032]; P=0.0003).

The change in thoracic volume per breath relative to thoracic volume increased with V_T (l kg^{-1}) in humans (slope±*S.* 1.72±0.30, 95% CI [1.12, 2.31], R^2=0.37) and weakly but significantly in dogs (0.29±0.49, 95% CI [−0.66, 1.24], R^2=0.03; P=0.0146; Fig. 4). Conversely, the change in thoracic volume decreased with increasing V_T (l kg^{-1}) in goats (−1.30±0.61, 95% CI [−2.50, −0.11], R^2=0.53), unlike humans (P<0.0001) and dogs (P=0.0445; Fig. 4). A small difference was observed in resting thoracic volume change relative to thoracic volume between humans (mean±s.e.m. 0.041±0.006; 95% CI [0.026, 0.006]) and dogs (0.057±0.010; 95% CI [0.016, 0.100]; P=0.3498), while larger differences were observed between goats (0.004±0.002; 95% CI [−0.006, 0.014])

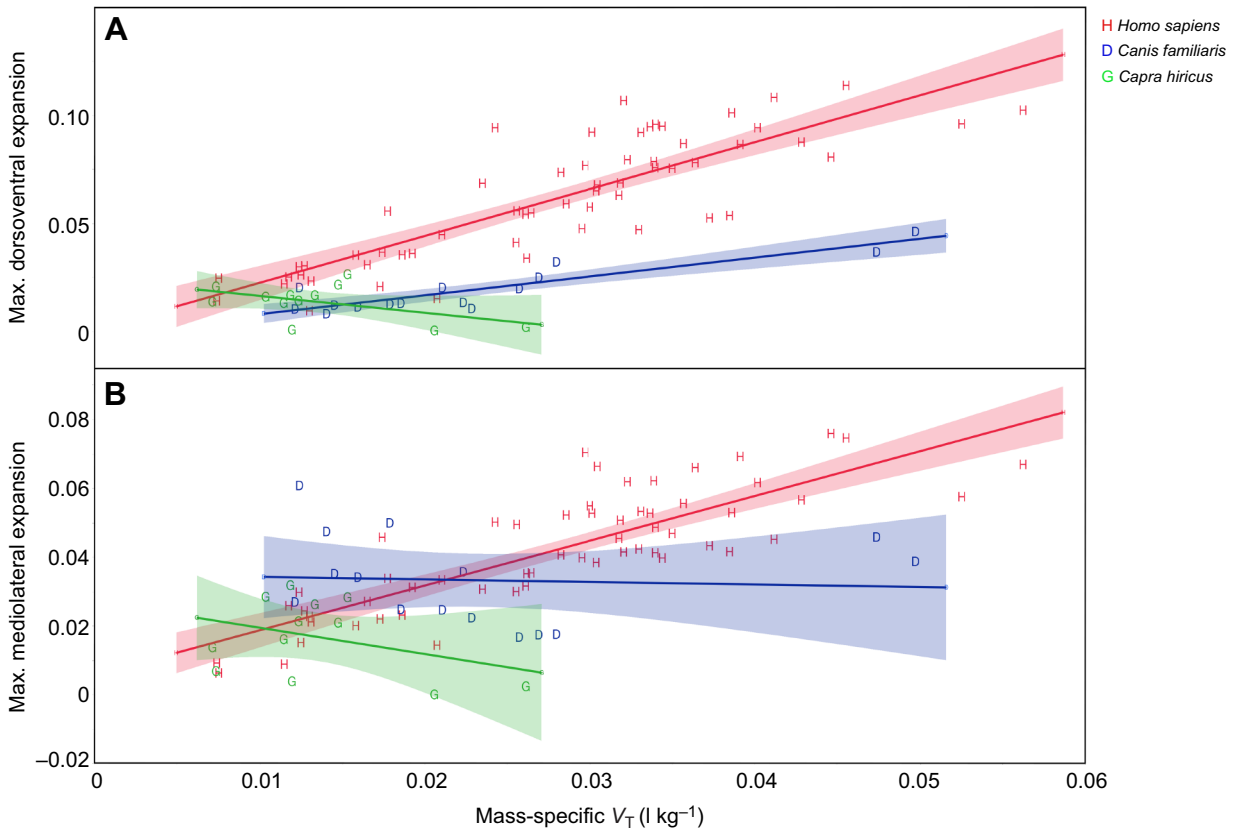

Fig. 3. Maximum dorsoventral thoracic expansion and maximum mediolateral thoracic expansion relative to mass-specific V_T in humans, dogs and goats. (A) Maximum dorsoventral thoracic expansion increased with V_T (l kg^{-1}) in humans and in dogs, but decreased in goats with increasing V_T (l kg^{-1}). (B) Maximum mediolateral thoracic expansion increased with V_T (l kg^{-1}) in humans but decreased weakly in dogs and strongly in goats with increasing V_T (l kg^{-1}). Expansion values are given relative to chest depth (A) and width (B). Shading represents 95% confidence interval (CI).

Journal of Experimental Biology (2019) 222, jeb189357. doi:10.1242/jeb.189357

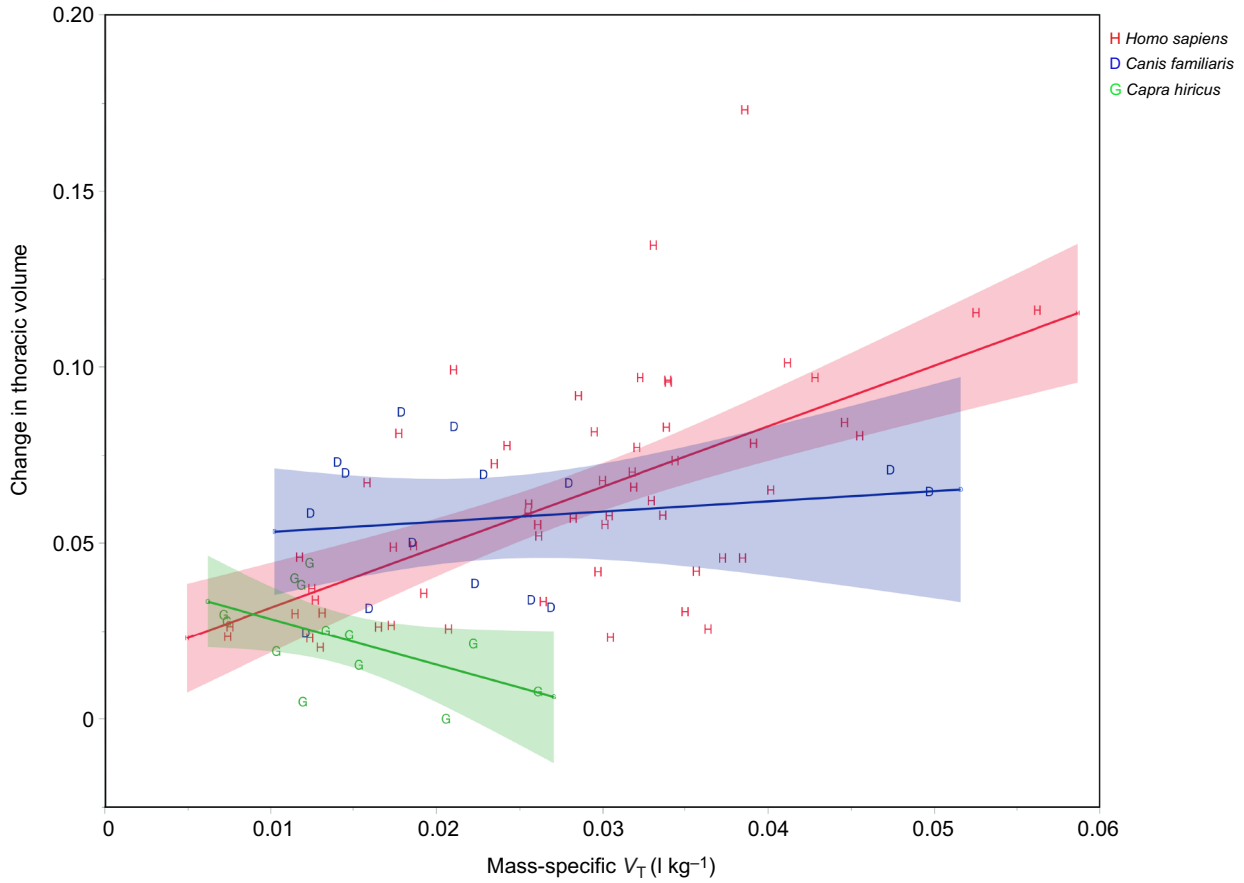

Fig. 4. Change in thoracic volume during ventilation with change in mass-specific V_T in humans, dogs and goats. Change in thoracic volume during ventilation increased in humans and weakly in dogs (P=0.0146) as V_T (l kg^{-1}) increased. Change in thoracic volume decreased in goats and was significantly different from that in humans (P<0.0001) and dogs (P=0.0445). Shading represents 95% CI.

and humans (P=0.0247) and between goats and dogs (P=0.0085). Overall, humans and dogs showed larger thoracic expansion and contraction relative to thoracic volume than goats. Both humans and dogs increased change in thoracic volume during ventilation when exercising, though humans more so (Fig. 4).

Costovertebral joint morphology in non-hominids

Within each order examined, cursorial species identified as endurance adapted had more concavo-convex costovertebral joint elements than related species identified as non-endurance and non-cursorial, which have flatter joints (Fig. 5; Fig. S2). Within carnivores, canines had joint elements that were approximately 3–10 times more concavo-convex than those of bears. Within perissodactyls, horses had joint elements that were approximately 2–15 times more concavo-convex than those of rhinoceroses. Finally, within artiodactyls, camels had joint elements that were approximately 2–14 times more concavo-convex than those of goats (and at least 4 times more concavo-convex than those of *Merycoidodon culbertsoni*, an extinct short-limbed, non-cursorial camel relative; Fig. S3, Table S3).

Significant differences in included angle of the joint elements between species identified as endurance-adapted cursors, non-endurance cursors and non-cursors within the same order were observed (Table 1; Table S3). We found that the curvature of the rib portions of joints was strongly correlated to that of vertebrae in the lower (P<0.0001, R^2=0.77) and upper (P<0.0001, R^2=0.66) portions of the joint in endurance-adapted cursorial species (Fig. 5). In non-endurance and non-cursorial species, the curvature of the rib portions of the joint was weakly correlated to that of vertebrae in the upper portion of the joint (P<0.0001, R^2=0.31), but not in the lower portion of the joint (R^2=0.0; Fig. 5).

Costovertebral joint morphology in hominids

Homo sapiens had joint elements that were 11–51 times more concavo-convex than those of *P. troglodytes* (P<0.0001; Figs 5 and 6; Fig. S2; Tables 1 and 2). *Australopithecus afarensis* joint facets were not significantly different from those of chimpanzees (superior costal facet, P=1.00; inferior costal facet, P=0.9986), nor were those of *Au. sediba* (superior costal facet, P=0.9999; inferior costal facet, P=0.9726; superior articular facet, P=0.9932; inferior articular facet, P=1.00; Table 2, Fig. 6). *Homo sapiens* costovertebral joint elements were considerably more concavo-convex than those of *Au. afarensis* (superior costal facet, P=0.0001; inferior costal facet, P=0.0033), and 12–69 times more concavo-convex than those of *Au. sediba* (superior costal facet, P<0.0001; inferior costal facet, P<0.0001; superior articular facet, P=0.0094; inferior articular facet, P=0.0087; Table 2, Fig. 6).

Homo erectus showed the same distinctive configuration as *H. sapiens*, with convex vertebral facets (superior costal facet, P=0.9274; inferior costal facet, P=0.9996) and concave rib facets (inferior articular facet, P=0.9995; Fig. 6). *Homo erectus* had joint elements that were more concavo-convex than those of *Au. afarensis* (superior costal facet, P=0.0048; inferior costal facet, P=0.0077), approximately 15–72 times more concavo-convex than those of *Au. sediba* (superior costal facet, P=0.0002;

Journal of Experimental Biology (2019) 222, jeb189357. doi:10.1242/jeb.189357

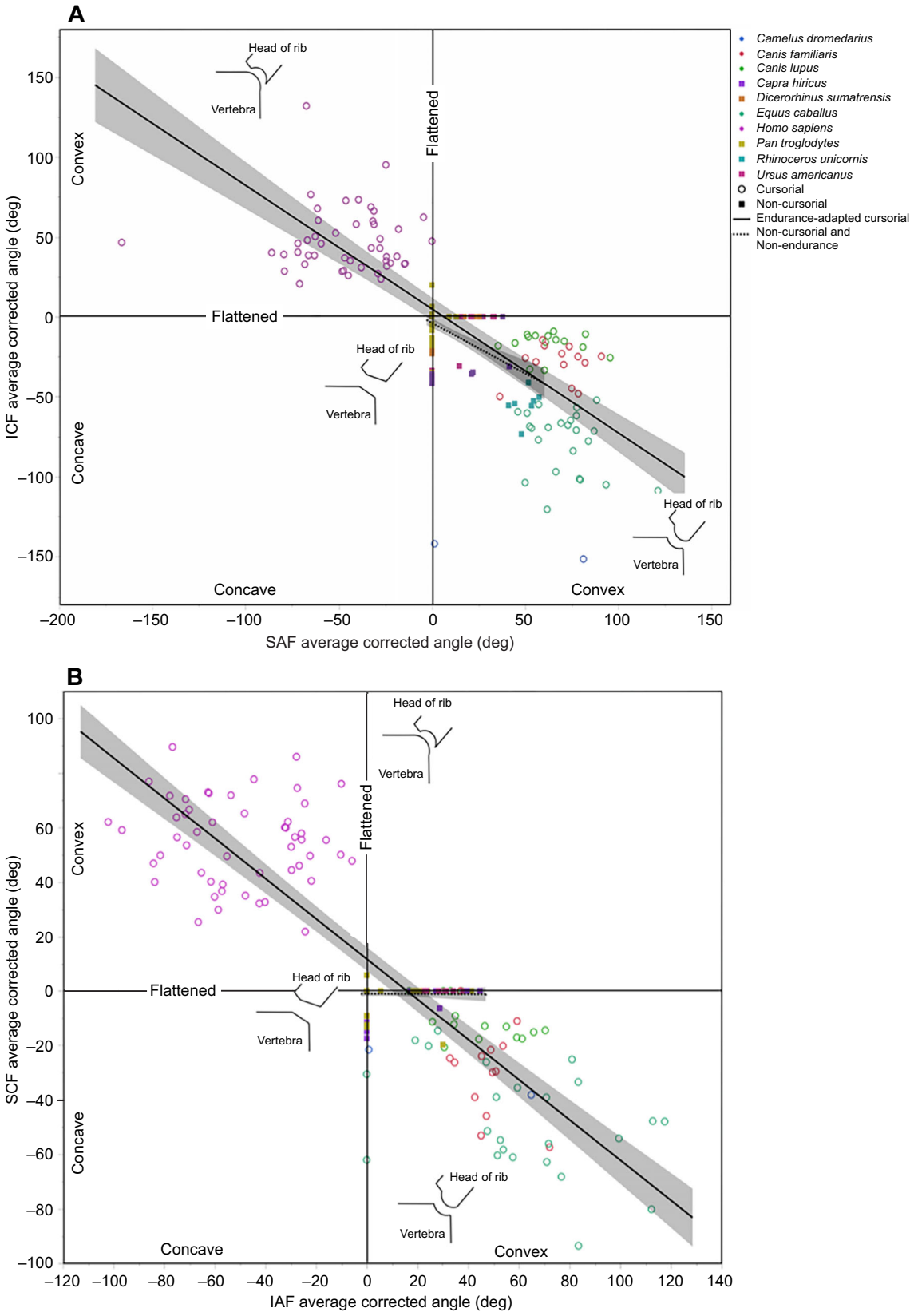

Fig. 5. Relationship between rib and vertebral elements of the costovertebral joint in endurance-adapted cursorial species and non-endurance or non-cursorial species. Endurance-adapted cursorial species exhibit greater joint facet curvature than non-endurance and non-cursorial species within the same order (indicated by color) in the upper portion (A) and lower portion (B) of the costovertebral joint. Rib facet included angle corresponds strongly with vertebral facet included angle in endurance-adapted cursorial specimens, but not in non-endurance and non-cursorial specimens. Negative values for the included angle indicate concave joint facets, while positive values indicate convexity. Larger values are associated with greater joint concavo-convexity. Angle values of 0 indicate a flat facet. ICF, inferior costal facet; SAF, superior articular facet; SCF, superior costal facet; and IAF, inferior articular facet.

Journal of Experimental Biology (2019) 222, jeb189357. doi:10.1242/jeb.189357

Table 1. Differences in inferior costal facet (ICF), superior articular facet (SAF), superior costal facet (SCF) and inferior articular facet (IAF) curvature between species within the same order

Comparison	Facet	Difference in average facet included angle (deg)	Cohen's *d*	Effect size
Modern human vs chimpanzee (Primates)	ICF	49.59±2.83 (*P*<0.0001)*	0.98	Large
	SAF	46.70±3.71 (*P*<0.0001)*	0.93	Large
	SCF	55.71±2.32 (*P*<0.0001)*	1.11	Very large
	IAF	54.22±3.75 (*P*<0.0001)*	1.08	Very large
Horse vs rhinoceros (Perissodactyla)	ICF	45.67±4.83 (*P*<0.0001)*	0.91	Large
	SAF	41.92±6.12 (*P*<0.0001)*	0.83	Large
	SCF	47.52±3.97 (*P*<0.0001)*	0.94	Large
	IAF	56.89±6.49 (*P*<0.0001)*	1.13	Very large
Camel vs goat (Artiodactyla)	ICF	129.49±4.83 (*P*<0.0001)*	2.57	Huge
	SAF	54.95±11.83 (*P*=0.0001)*	1.09	Large
	SCF	9.43±3.97 (*P*=0.8890)	0.19	Small
	IAF	21.60±14.58 (*P*=0.9870)	0.43	Medium
Canine vs bear (Carnivora)	ICF	21.20±4.04 (*P*<0.0001)*	0.42	Medium
	SAF	55.60±5.23 (*P*<0.0001)*	1.11	Very large
	SCF	19.73±3.32 (*P*=0.0047)*	0.39	Medium
	IAF	33.51±5.43 (*P*<0.0001)*	0.66	Medium

Angles are means±s.e.m. Effect size data are from Cohen (1988) and Sawilowsky (2009). *Significant difference (P<0.05) between species of the same order.

inferior costal facet, P<0.0001; inferior articular facet, P=0.1788), and approximately 12–46 times more concavo-convex than those of chimpanzees (superior costal facet, P<0.0001; inferior costal facet, P<0.0001; inferior articular facet, P=0.0700; Table 2, Fig. 6).

Finally, *H. neanderthalensis* specimens exhibited a costovertebral joint morphology similar to that of other species of the genus *Homo*. Like *H. sapiens*, *H. neanderthalensis* had convex vertebral facets (superior costal facet, P=0.3986; inferior costal facet, P=0.2957) and concave rib facets (inferior articular facet, P=0.7616; superior articular facet, P=0.3329). *Homo neanderthalensis* joint elements were more concavo-convex than those of *Au. afarensis* (superior costal facet, P=0.0064; inferior costal facet, P=0.1094), approximately 4–49 times more concavo-convex than those of *Au. sediba* (superior costal facet, P=0.0002; inferior costal facet, P=0.0020; inferior articular facet, P=0.3586; superior articular facet, P=0.6509), and approximately 7–41 times more concavo-convex than those of chimpanzees (superior costal facet, P<0.0001; inferior costal facet, P=0.0012; inferior articular facet, P=0.1459; superior articular facet, P=0.3028; Table 2, Fig. 6).

DISCUSSION

Aerobically demanding and sustained activities such as long-distance running require increased air intake. Here, we first experimentally tested whether two species that independently evolved adaptations for endurance cursoriality (humans and dogs) augment diaphragmatic contributions to inspiration by increasing thoracic ventilation relative to V_T during locomotion in comparison with a non-endurance species (goats). To make this comparison, we measured total thoracic volume change with increasing f_H and changing V_T. We found that humans had the ability to increase the amount of overall thoracic expansion and contraction per breath as V_T increased (Fig. 4) through increased dorsoventral and mediolateral expansion (Fig. 3). Dogs maintained almost the same amount of overall volumetric expansion and contraction of the thorax as V_T increased (Fig. 4), but they increased dorsoventral expansion to increase V_T (Fig. 3). Goats, however, had limited thoracic expansion during respiration (Fig. 3), with less thoracic expansion and contraction per breath as V_T increased (Fig. 4).

We also observed that human and dog thoraxes functioned differently, as predicted, in terms of mediolateral expansion. As V_T increased, humans increased the amount of both dorsoventral and mediolateral thoracic expansion per breath. In contrast, dogs only increased dorsoventral expansion, and to a lesser extent than in humans. Dogs also slightly decreased mediolateral expansion as they increased V_T, accounting for the differences in overall thoracic expansion observed between humans and dogs. The observed lack of increase in mediolateral expansion per breath with larger V_T suggests that mediolateral thoracic expansion generated by BH rib motion is limited in dogs, which represent an intermediate between humans and goats.

This limitation may extend to other cursorial quadrupeds for several reasons. First, endurance-adapted cursors, like dogs and horses, have greater $\dot{V}_{O_2,max}$ than expected for their body mass (Poole and Erickson, 2011). This ability to effectively and efficiently transport oxygen into the body, along with the ability to increase the volume of the thorax via thoraco-abdominal elongation during trotting and galloping (Marlin et al., 2002), may have reduced selection for increased thoracic expansion during ventilation while aerobically active. Simply put, quadrupedal endurance-adapted cursors like dogs may not need to rely on mediolateral thoracic expansion to increase the volume of the thorax. The observed increase in dorsoventral expansion, and the resulting change in overall thoracic volume, may suffice.

Second, cursorial quadrupeds need to support their body weight with their forelimbs by keeping each forelimb in a parasagittal plane. As described in horses (McGuigan and Wilson, 2003; Beck and Clayton, 2013) and dogs (Carrier et al., 2006), the trunk of cursorial quadrupeds is suspended between the forelimbs by a muscular thoracic sling (Kardong, 1998). Portions of this thoracic sling, including the m. serratus ventralis, directly connect the cervical transverse processes and sternal ribs to the dorsomedial aspect of the scapula and control the position of the scapulae relative to the thorax (Davis, 1949; Gray, 1968; Beck and Clayton, 2013). BH motion of the sternal ribs and the resulting mediolateral thoracic expansion would therefore cause mediolateral motion of the scapula during locomotion because the scapula attaches directly to the dorsolateral surface of the rib cage. Decreased movement in the parasagittal plane may increase the stability of the shoulder during locomotion and may be resisted by force imposed by the limb.

Finally, another likely explanation for the reduced mediolateral thoracic expansion in dogs is the typical shape of the quadrupedal

Journal of Experimental Biology (2019) 222, jeb189357. doi:10.1242/jeb.189357

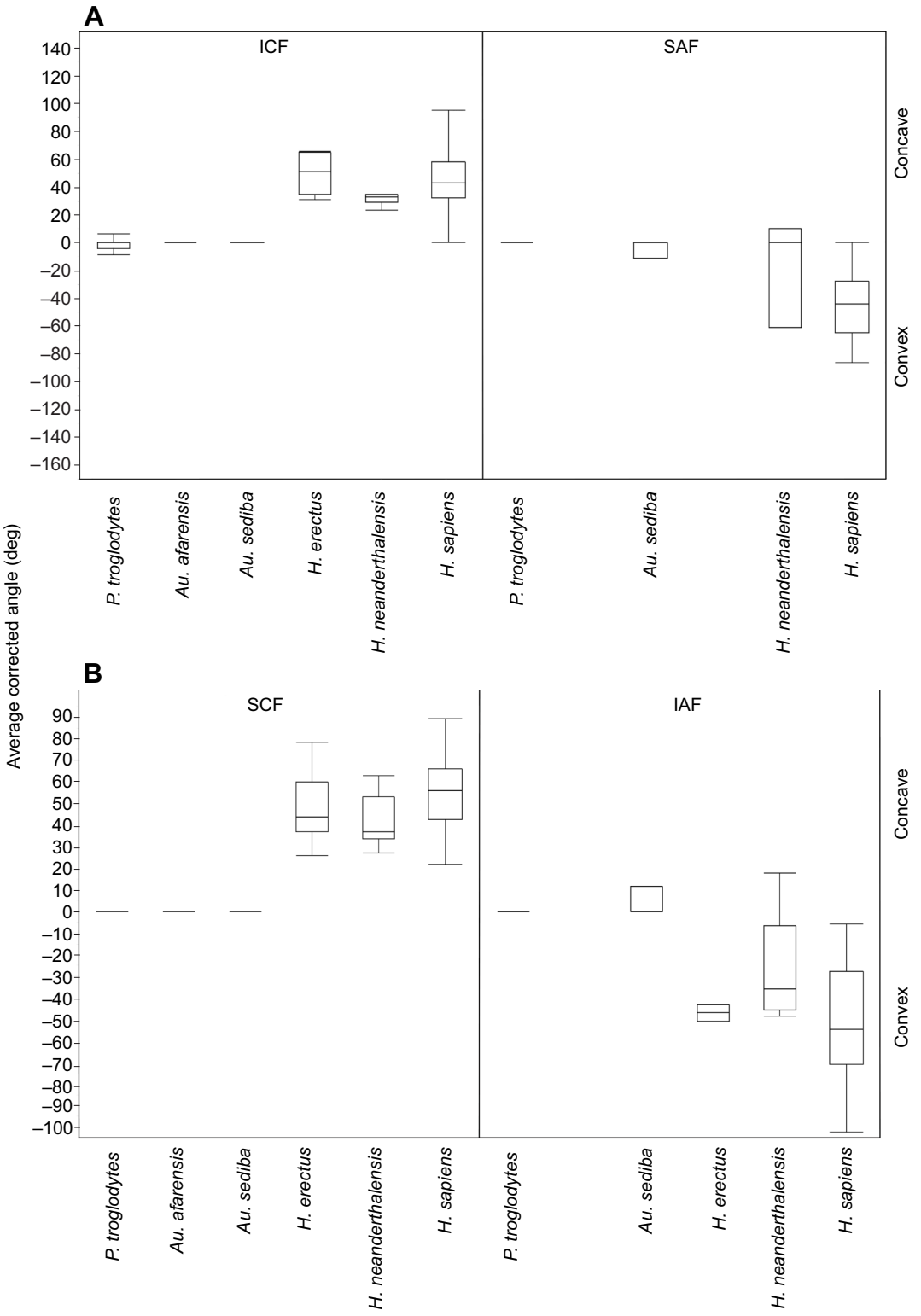

Fig. 6. Differences in costovertebral joint morphology among hominid species. (A) Superior and (B) inferior sites of articulation. Australopiths exhibit a chimpanzee-like joint morphology whereas *Homo* species are all similar in morphology but differ from that of chimpanzees. Negative values for the included angle indicate concave joint facets, while positive values indicate convexity. Larger values are associated with greater joint concavo-convexity. Angle values of 0 indicate a flat facet. ICF, inferior costal facet; SAF, superior articular facet; SCF, superior costal facet; IAF, inferior articular facet.

cursor thorax. Most cursorial mammals have evolved deep and narrow rib cages with shortened costal cartilage and ribs that are highly flattened mediolaterally (Hildebrand, 1988; Bramble, 1989), thereby reducing the lateral curvature of the chest and resulting in limited mediolateral expansion when the ribs swing upwards in the BH motion. This characteristic chest shape may have been selected for to reduce bending moments on the ribs during locomotion (Bramble, 1989). Thus, selection to reduce loading of the thorax

Journal of Experimental Biology (2019) 222, jeb189357. doi:10.1242/jeb.189357

Table 2. Measured costovertebral included angles across sampled hominids

Species	No. of specimens	ICF (deg)	SAF (deg)	SCF (deg)	IAF (deg)
Pan troglodytes	8	−3.35±1.87 (*N*=70)	0.410±2.55 (*N*=54)	−1.04±1.58 (*N*=56)	3.69±2.57 (*N*=54)
Australopithecus afarensis (AL-288)	1	0.00±11.08 (*N*=2)		0.00±8.35 (*N*=2)	
Australopithecus sediba (MH1 and MH2)	2	0.67±0.67 (*N*=14)	−3.82±10.84 (*N*=3)	0.00±3.94 (*N*=9)	3.95±10.90 (*N*=3)
Homo erectus (KNM-WT15000)	1	48.26±5.92 (*N*=7)		47.78±4.82 (*N*=6)	−47.06±13.35 (*N*=2)
Homo neanderthalensis (Shanidar 2, Shanidar 3, Dederiyeh 2)	3	32.94±5.54 (*N*=8)	−17.11±10.84 (*N*=3)	41.34±4.47 (*N*=7)	−28.02±8.44 (*N*=5)
Homo sapiens	9	46.24±1.87 (*N*=70)	−46.29±2.7 (*N*=47)	54.67±1.58 (*N*=56)	−50.56±2.62 (*N*=52)

ICF, inferior costal facet; SAF, superior articular facet; SCF, superior costal facet; and IAF, inferior articular facet. Angles are means±s.e.m. Negative values for the included angle indicate concave joint facets, while positive values indicate convexity. Larger values are associated with greater joint concavo-convexity. Angle values of 0 indicate a flat facet.

has resulted in a rib shape that also limits BH motion, and therefore mediolateral thoracic expansion. However, the thoracic structure typical of quadrupedal cursors is not observed in bipedal cursors, such as humans and kangaroos (Bramble, 1989), which have more laterally curved chests, so when the ribs swing upwards in these species there is a larger change in the lateral dimension of the thorax. Thus, more BH motion and mediolateral thoracic expansion occur.

Unlike in quadrupedal cursors, which rely on thoraco-abdominal elongation to increase V_T during galloping and trotting (Marlin et al., 2002), thoraco-abdominal elongation during locomotion may be constrained in humans, who walk and run bipedally with the thoracic cavity positioned above the abdominal viscera. Because humans do not rely on a thoracic sling to support the forelimbs and because the human thorax does not follow the typical cursorial thoracic bauplan, bipedalism allows for increased mediolateral and dorsoventral thoracic expansion of the thorax. Thus, to compensate for restrictions on increasing thoracic volume cranial–caudally due to bipedality, we hypothesize that humans rely on both greater dorsoventral expansion and greater mediolateral expansion to increase the volume of the thorax during aerobic ventilation. However, as in quadrupeds, increased rib mobility and thoracic movement likely involves a tradeoff between stability and increased ventilatory ability. The configuration of the upper thorax and scapula in chimpanzees has been argued to be associated with arboreal locomotion in order to resist large bending moments generated by contraction of the thoracoscapular muscles (Hunt, 1991; Preuschoft, 2004). Furthermore, trunk stability and increased stiffness of proximal muscle attachments may improve muscle force production in the extremities needed for quick and powerful movements (Hodges et al., 1997; Jensen et al., 2000). Increased rib mobility may require increased respiratory muscle activation and increasing intrathoracic pressure to stabilize the rib cage during arboreal locomotion and may reduce the ability of the ribs to resist bending moments during arm loading. Thus, thoracic mobility and thoracic expansion may have been constrained in hominins such as australopiths that continued to rely on arboreal climbing.

Based on our data, if the modern human thorax were as constrained in terms of expansion as a goat's, a 71 kg (average body mass of this study's participants) human's maximum V_T would be approximately 2.25 l, around 47% of typical human vital capacity and approximately 79% of the average maximum V_T (2.84 l) measured in our human participants. In addition, maximum $\dot{V}_E$ (l min^{-1} kg^{-1}) would be reduced to 1.97 l min^{-1} kg^{-1} (based on an observed maximum respiration rate of 62 breaths min^{-1}), an approximate 9% reduction in the maximum measured $\dot{V}_E$.

Our experimental results predict greater costovertebral concavo-convexity in humans and dogs than in goats. As expected, we found that humans and dogs have 2–10 times more concavo-convex costovertebral joint elements than goats. Based on this finding, endurance-adapted cursorial species should have more concavo-convex articular facets on the ribs and bodies of the vertebrae than closely related non-endurance and non-cursorial species. Increased joint concavo-convexity should permit greater rotation around the ribs' long axes and more flexion for increased dorsoventral and mediolateral thoracic expansion as a result of more BH and PH motion, respectively. We found that endurance-adapted cursorial species have 2–51 times more concavo-convex costovertebral joint elements than non-endurance and non-cursorial species from the same order, which have flatter joints (Fig. 5; Fig. S2). In particular, humans have joint elements that are more concavo-convex than those of chimpanzees, canids have joint elements that are more concavo-convex than those of bears, horses have joint elements that more concavo-convex than those of rhinoceroses, and camels have joint elements that are more concavo-convex than those of goats (and more concavo-convex than those of a non-cursorial ancestor, *Merycoidodon*; Fig. S3, Table S3). Given that mammals, unlike reptiles, ventilate while they locomote and that endurance-adapted cursorial species have more concavo-convex costovertebral joint elements (from which rib movements originate), increased joint concavo-convexity likely indicates the ability of the thorax to undergo larger expansion and contraction during each breath using dorsoventral expansion either alone or in conjunction with mediolateral expansion.

Based on the measured differences in joint morphology across taxa, it appears that the costovertebral joint has been subject to convergent selective pressure across several orders to facilitate increased sustained aerobic capacity. The observation that increased costovertebral concavo-convexity is present to some extent in all the endurance-adapted cursorial species surveyed and is lacking in non-endurance and non-cursorial species suggests that increased joint curvature helps facilitate large V_T that, along with changes in f_R, are necessary for long-distance running. Furthermore, comparisons of extant camels and *Merycoidodon*, a short-limbed non-cursorial terrestrial ancestor of camels (Clifford, 2010), suggest that increased concavo-convexity was selected for following the evolution of endurance cursoriality in camelids (Fig. S3). As one might predict from convergent evolution, the pattern of increased concavo-convexity differs in some of these cursorial species. Camels show increased curvature of the upper portion of the costovertebral joint relative to that of goats and *Merycoidodon*, with an almost ball-and-socket configuration. Furthermore, whereas the rib facets of the joint are convex and the vertebral facets are concave in endurance-adapted cursorial carnivores, artiodactyls and perissodactyls, this pattern is reversed in humans, with concave rib facets and convex vertebral

facets (Fig. 5; Fig. S2). We infer that humans independently evolved a novel costovertebral joint architecture to facilitate increased thoracic expansion and contraction, and hence V_T, during sustained long-distance bipedal running. As with many other skeletal adaptations for running, this shift appears to coincide with the origins of the genus *Homo* (Bramble and Lieberman, 2004). Together, these morphological data and kinematic experiments support the hypothesis that humans, like dogs and other endurance-adapted cursorial species, independently experienced selection to increase thoracic volumetric change during aerobic respiration by increasing the concavo-convexity of the costovertebral joints, which, in turn, permits greater dorsoventral and mediolateral thoracic expansion (from increased PH and BH motion, respectively) to increase V_T as needed.

This study has several limitations. First, the costovertebral joint can be subject to damage and deterioration in fossil samples, making measurements approximate. We found the heads of ribs in Neanderthal specimens to be especially damaged. Second, our study only compared thoracic ventilation between three species, only two quadrupedal species were studied experimentally, and sample sizes were small because of the limited number of available subjects. Future studies should include a wider variety of cursorial and non-cursorial species and more subjects. Furthermore, limitations on subject training constrained the speed at which we could safely run the dogs and goats. As such, thoracic ventilation in goats and dogs was only measured while the animals rested, walked and trotted. Thus, our results do not reflect how the thorax might function during galloping in quadrupeds, which may be different from that during walking and trotting as a result of dissimilarities in entrainment and respiratory mechanics between gaits (Bramble and Carrier, 1983; Bramble, 1989; Boggs, 2002). However, cursorial quadrupeds use thoraco-abdominal elongation to expand the thoracic cavity and increase V_T, with both thoraco-abdominal elongation (Marlin et al., 2002) and V_T (Szlyk et al., 1981) increasing most during galloping. This increase in thoracic volume, coupled with highly efficient cardiovascular and muscular systems and high $\dot{V}_{O_2}$ (Poole and Erickson, 2011), makes it unlikely that cursorial animals would increase thoracic ventilation only during trotting and not during galloping, though this is a topic for future research. Third, our goat subjects may have been stressed when measured at rest, resulting in possibly inflated measurements of resting V_T or f_R relative to previous studies (Smith et al., 1983). However, because the purpose of this study was to measure the relationship between thoracic ventilation and V_T, potentially larger or faster breaths taken by our goats at rest would not affect our conclusions. Fourth, the use of surface markers can lead to errors in kinematic measurements because of the motion of the skin and underlying subcutaneous fat. Future experiments using X-ray reconstruction of moving morphology (XROMM) would provide more accuracy and precision. We are nonetheless confident in our results because we used multiple markers to measure changes in thoracic volume during expansion and contraction across multiple breaths and because we attempted to limit the amount of extraneous marker motion (Fig. 2). Fifth, costovertebral joint movement itself was not measured, but rather inferred from overall thoracic expansion and contraction. XROMM experiments could shed light on how the joint itself moves during locomotion. Finally, chest shape and size vary among humans, and the human participants in this study were selected from college-age males living at sea level. Thus, another avenue for future research is to test whether there are any differences in thoracic expansion patterns between males and females and among populations with long-term exposure to high elevation.

Although more research is needed to test the relationship between costovertebral morphology and thoracic movement during high-intensity aerobic activity, the above results in combination with morphological measurements on costovertebral joints in the hominin fossil record allow us to speculate about selection for enhanced ventilatory capacity in human evolution. While thoracic size influences overall respiratory volume, our results suggest that rib mobility is also a key feature of aerobic respiration. As noted above, modern humans have a unique costovertebral joint morphology in which the rib facets of the costovertebral joint are convex and the vertebral facets are concave (Fig. 5; Fig. S2). This unique joint morphology appears occur in all species of the genus *Homo* (though there is increased variation in the articular facets of *H. neanderthalensis*, likely due to wear and damage common in fossil ribs) but is lacking in australopiths and great apes (Fig. 6). Because lung volume scales isometrically with body mass in mammals (interspecific slope=1.06; Gehr et al., 1981), we can approximate thoracic volume changes in hominin species based on estimated body mass and assuming modern human-like dorsoventral and mediolateral thoracic expansion from costovertebral joint shape. Using an estimated body mass of 51.4 kg (Grabowski et al., 2015) and assuming similar thoracic motion to that of modern humans, we estimate that *H. erectus* would have had a thoracic volume change during inspiration and expiration at $f_{H,max}$ approximately 0.27 l greater than that of a similar-sized chimpanzee, resulting in an additional oxygen intake of 16.73 l min^{-1} from increased thoracic ventilation alone. Although $\dot{V}_{O_2,max}$ is affected by muscle fiber composition (Bergh et al., 1978), mitochondrial density and other variables that are modified by aerobic training (Astrand and Rodahl, 1986), we can nonetheless approximate the effect of increased thoracic motion on *H. erectus* $\dot{V}_{O_2,max}$. By calculating expected $\dot{V}_{O_2,max}$ from body mass (M_B; Calder, 1981) for an average chimpanzee male ($\dot{V}_{O_2,max}$=2.2 l min^{-1}, M_B=39 kg), calculating expected $\dot{V}_{O_2,max}$ for a 71 kg modern human male ($\dot{V}_{O_2,max}$=3.564 l min^{-1}), and comparing these values with the measured average $\dot{V}_{O_2,max}$ in modern human males ($\dot{V}_{O_2,max}$=4.5 l min^{-1}; Bergh et al., 1978), we estimate that *H. erectus* had a $\dot{V}_{O_2,max}$ of approximately 3.8 l min^{-1}, around 38% greater than the expected $\dot{V}_{O_2,max}$ calculated from body mass alone. We therefore conclude that the derived human-like costovertebral joint morphology evolved in response to increased selection for high aerobic capacity activities such as endurance running in *Homo* approximately 2 million years ago.

Acknowledgements

We thank the Harvard Museum of Comparative Zoology, the Peabody Museum of Archaeology and Ethnology and the National Museum of Natural History for access to collections. Statistical support was provided by data science specialist Steven Worthington at the Institute for Quantitative Social Science, Harvard University. We also thank the members of the Skeletal Biology and Biomechanics Lab, especially Ian Wallace and Heidi Nocka, for helping with data collection. We thank the five anonymous reviewers who provided comments that greatly improved the quality of the manuscript. Finally, a special thank you to the humans, animals and dog-owners that participated in these experiments.

Competing interests

The authors declare no competing or financial interests.

Author contributions

Conceptualization: W.É.C., D.E.L.; Methodology: W.É.C., D.E.L.; Validation: W.É.C.; Formal analysis: W.É.C., N.B.H.; Investigation: W.É.C., N.B.H.; Resources: D.E.L.; Writing - original draft: W.É.C., N.B.H., D.E.L.; Visualization: W.É.C., D.E.L.; Supervision: D.E.L.; Project administration: D.E.L.; Funding acquisition: D.E.L.

Funding
This research received no specific grant from any funding agency in the public, commercial or not-for-profit sectors.

Data availability
Data are available from the Dryad digital repository (Callison et al., 2019): doi.org/10.5061/dryad.9zw3r2299

Supplementary information
Supplementary information available online at
http://jeb.biologists.org/lookup/doi/10.1242/jeb.189357.supplemental

References

Aiello, L. and Dean, C. (1990). *An Introduction to Human Evolutionary Anatomy*. New York: Academic Press.
Astrand, P. and Rodahl, K. (1986). *Textbook of Work Physiology*. New York: McGraw-Hill.
Barrentine, L. B. (1991). *Concepts for R&R Studies*. Milwaukee, WI: ASQ Quality Press.
Bastir, M., García-Martínez, D., Williams, S. A., Recheis, W., Torres-Sánchez, I., García Río, F., Oishi, M. and Ogihara, N. (2017). 3D geometric morphometrics of thorax variation and allometry in Hominoidea. *J. Hum. Evol.* **113**, 10-23. doi:10.1016/j.jhevol.2017.08.002
Beck, W. and Clayton, H. (2013). *Equine Locomotion*, 2nd edn. Philadelphia: Saunders.
Bergh, U., Thorstensson, A., Sjodin, B., Hulten, B., Piehl, K. and Karlsson, J. (1978). Maximal oxygen uptake and muscle fiber types in trained and untrained humans. *Med. Sci. Sports* **10**, 151-154.
Berry, M. J., Dunn, C. J., Pittman, C. L., Kerr, W. C. and Adair, N. E. (1996). Increased ventilation in runners during running as compared to walking at similar metabolic rates. *Eur. J. Appl. Physiol. Occup. Physiol.* **73**, 245-250. doi:10.1007/BF02425483
Boggs, D. F. (2002). Interactions between locomotion and ventilation in tetrapods. *Comp. Biochem. Physiol. A* **133**, 269-288. doi:10.1016/S1095-6433(02)00160-5
Brainerd, E. L., Mortiz, S. and Ritter, D. A. (2016). XROMM analysis of rib kinematics during lung ventilation in the green iguana, *Iguana iguana*. *J. Exp. Biol.* **219**, 404-411. doi:10.1242/jeb.127928
Bramble, D. M. (1989). Axial-appendicular dynamics and the integration of breathing and gait in mammal. *Am. Zool.* **29**, 171-186. doi:10.1093/icb/29.1.171
Bramble, D. M. and Carrier, D. (1983). Running and breathing in mammals. *Science* **219**, 251-256. doi:10.1126/science.6849136
Bramble, D. M. and Jenkins, F. A. (1993). Mammalian locomotor-respiratory integration: implications for diaphragmatic and pulmonary design. *Science* **262**, 235-240. doi:10.1126/science.8211141
Bramble, D. M. and Lieberman, D. E. (2004). Endurance running and the evolution of Homo. *Nature* **432**, 345-352. doi:10.1038/nature03052
Brocklehurst, R. J., Moritz, S., Codd, J., Sellers, W. I. and Brainerd, E. (2017). Rib kinematics during lung ventilation in the American alligator (Alligator mississippiensis): an XROMM analysis. *J. Exp. Biol.* **220**, 3181-3190. doi:10.1242/jeb.156166
Bulbulian, R., Wilcox, A. and Darabos, B. (1986). Anaerobic contribution to distance running performance of trained cross-country athletes. *Med. Sci. Sport Exercise* **18**, 107-113. doi:10.1249/00005768-198602000-00018
Calder, W. A. (1981). Scaling of physiological processes in homeothermic animals. *Annu. Rev. Physiol.* **43**, 301-322. doi:10.1146/annurev.ph.43.030181.001505
Callison, W. É., Holowka, N. B. and Lieberman, D. E. (2019). Thoracic adaptations for ventilation during locomotion in humans and other mammals. Dryad Digital Repository. doi:10.5061/dryad.9zw3r2299
Carrano, M. T. (1999). What, if anything, is a cursor? Categories versus continua for determining locomotor habit in mammals and dinosaurs. *J. Zool.* **247**, 29-42. doi:10.1111/j.1469-7998.1999.tb00190.x
Carrier, D. (1991). Conflict in the hypaxial musculo-skeletal system: documenting an evolutionary constraint. *Am. Zool.* **31**, 644-654. doi:10.1093/icb/31.4.644
Carrier, D. (1996). Function of the intercostal muscles in trotting dogs: ventilation or locomotion? *J. Exp. Biol.* **199**, 1455-1465.
Carrier, D. R., Kapoor, A. K., Kimura, T., Nickels, M. K., Scott, E. C., So, J. K. and Trinkaus, E. (1984). The energetic paradox of human running and hominid evolution [and Comments and Reply]. *Curr. Anthropol.* **25**, 483-495. doi:10.1086/203165
Carrier, D. R., Deban, S. M. and Fischbein, T. (2006). Locomotor function of the pectoral girdle 'muscular sling' in trotting dogs. *J. Exp. Biol.* **209**, 2224-2237. doi:10.1242/jeb.02236
Clifford, A. B. (2010). The evolution of the unguligrade manus in artiodactyls. *J. Vertebr. Paleontol.* **30**, 1827-1839. doi:10.1080/02724634.2010.521216
Codd, J. R., Boggs, D. F., Perry, S. F. and Carrier, D. R. (2005). Activity of three muscles associated with the uncinate processes of the giant Canada goose *Branta canadensis maximus*. *J. Exp. Biol.* **208**, 849-857. doi:10.1242/jeb.01489
Cohen, J. (1988). *Statistical Power Analysis for the Behavioral Sciences*. New Jersey: Routledge.
Colborne, G. R., Allen, R. J., Wilson, R. J. R., Marlin, D. J. and Franklin, S. H. (2006). Thoracic geometry changes during equine locomotion. *Equine Comp. Exercise Physiol.* **3**, 53-59. doi:10.1079/ECP200686
Coombs, W. P. (1978). Theoretical aspects of cursorial adaptations in dinosaurs. *Q. Rev. Biol.* **53**, 393-418. doi:10.1086/410790
Da Silva, K. M., Sayers, B. M., Sears, T. A. and Stagg, D. T. (1977). The changes in configuration of the rib cage and abdomen during breathing in the anaesthetized cat. *J. Physiol.* **266**, 499-521. doi:10.1113/jphysiol.1977.sp011779
Daley, M. A., Bramble, D. M. and Carrier, D. R. (2013). Impact loading and locomotor-respiratory coordination significantly influence breathing dynamics in running humans. *PLoS ONE* **8**, e70752. doi:10.1371/journal.pone.0070752
Davis, D. (1949). The shoulder architecture of bears and other carnivores. *Fieldiana (Zoolology)* **31**, 285-305. doi:10.5962/bhl.title.1291
Dempsey, J. A. (1985). Is the lung built for exercise? *Med. Sci. Sports Exerc.* **18**, 143-155. doi:10.1249/00005768-198604000-00001
Dudar, J. C. (1993). Identification of rib number and assessment of intercostal variation at the sternal rib end. *J. Forensic Sci.* **38**, 788-797. doi:10.1520/JFS13474J
Franciscus, R. G. and Churchill, S. E. (2002). The costal skeleton of Shanidar 3 and a reappraisal of Neandertal thoracic morphology. *J. Hum. Evol.* **42**, 303-356. doi:10.1006/jhev.2001.0528
García-Martínez, D., Barash, A., Recheis, W., Utrilla, C., Torres Sánchez, I., García Río, F. and Bastir, M. (2014). On the chest size of Kebara 2. *J. Hum. Evol.* **70**, 69-72. doi:10.1016/j.jhevol.2014.02.003
Garland, T. (1983). The relation between maximal running speed and body mass in terrestrial mammals. *J. Zool.* **199**, 157-170. doi:10.1111/j.1469-7998.1983.tb02087.x
Gehr, P., Mwangi, D. K., Ammann, A., Maloiy, G. M. O., Taylor, C. R. and Weibel, E. R. (1981). Design of the mammalian respiratory system. V. Scaling morphometric pulmonary diffusing capacity to body mass: wild and domestic mammals. *Respir. Physiol.* **44**, 61-86. doi:10.1016/0034-5687(81)90077-3
Gómez-Olivencia, A., Eaves-Johnson, K. L., Franciscus, R. G., Carretero, J. M. and Arsuaga, J. (2009). Kebara 2: new insights regarding the most complete Neandertal thorax. *J. Hum. Evol.* **57**, 75-90. doi:10.1016/j.jhevol.2009.02.009
Grabowski, M., Hatala, K. G., Jungers, W. L. and Richmond, B. G. (2015). Body mass estimates of hominin fossils and the evolution of human body size. *J. Hum. Evol.* **85**, 75-93. doi:10.1016/j.jhevol.2015.05.005
Gray, J. (1968). *Animal Locomotion*. London: Weidenfeld and Nicolson.
Haile-Selassie, Y., Latimer, B. M., Alene, M., Deino, A. L., Gibert, L., Melillo, S. M., Saylor, B. Z., Scott, G. R. and Lovejoy, O. (2010). An early *Australopithecus afarensis* postcranium from Woranso-Mille, Ethiopia. *Proc. Natl. Acad. Sci. USA* **107**, 12121-12126. doi:10.1073/pnas.1004527107
Hamrick, M. W. (1996). Articular size and curvature as determinants of carpal joint mobility and stability in strepsirrhine primates. *J. Morphol.* **230**, 113-127. doi:10.1002/(SICI)1097-4687(199611)230:2<113::AID-JMOR1>3.0.CO;2-I
Hildebrand, M. (1988). *Analysis of Vertebrate Structure*, 4th edn. New York: Wiley & Sons.
Hodges, P. W., Butler, J. E., McKenzie, D. K. and Gandevia, S. C. (1997). Contraction of the human diaphragm during rapid postural adjustments. *J. Physiol.* **505**, 539-548. doi:10.1111/j.1469-7793.1997.539bb.x
Hunt, K. D. (1991). Mechanical implications of chimpanzee positional behavior. *Am. J. Phys. Anthropol.* **86**, 521-536. doi:10.1002/ajpa.1330860408
Jellema, L. M., Latimer, B. and Walker, A. (1993). The rib cage. In *The Nariokotome Homo erectus Skeleton* (ed. A. Walker and R. Leakey), pp. 294-325. Cambridge: Harvard University Press.
Jensen, B. R., Laursen, B. and Sjogaard, G. (2000). Aspects of shoulder function in relation to exposure demands and fatigue – a mini review. *Clin. Biomech.* **15**, S17-S20. doi:10.1016/S0268-0033(00)00054-1
Jordanoglou, J. (1970). Vector analysis of rib movement. *Respir. Physiol.* **10**, 109-120. doi:10.1016/0034-5687(70)90031-9
Kardong, K. V. (1998). *Vertebrates - Comparative Anatomy, Function, Evolution*. Boston: McGraw-Hill.
Kram, R. (1989). A treadmill mounted force platform. *J. Biomech.* **22**, 1041. doi:10.1016/0021-9290(89)90332-1
Latimer, B., Lovejoy, C. O. and Haile-Selassie, Y. (2016). The thoracic cage of KSD-VP-1/1. In *The Postcranial Anatomy of Australopithecus afarensis: New Insights KSD-VP-1/1Y* (ed. Y. Haile-Selassie and D. F. Su), pp. 143-154. Dordrecht: Springer.
Lindstedt, S. L., Hokanson, J. F., Wells, D. J., Swain, S. D., Hoppeler, H. and Navarro, V. (1991). Running energetics in the pronghorn antelope. *Nature* **353**, 748-750. doi:10.1038/353748a0
Lucas, A., Therminarias, A. and Tanche, M. (1980). Maximum oxygen consumption in dogs during muscular exercise and cold exposure. *Pflügers Arch. Eur. J. Physiol.* **388**, 83-87. doi:10.1007/BF00582633
Margulies, S. S., Rodarte, J. R. and Hoffman, E. A. (1989). Geometry and kinematics of dog ribs. *J. Appl. Physiol.* **67**, 707-712. doi:10.1152/jappl.1989.67.2.707

Marlin, D. J., Schroter, R. C., Cashman, P. M. M., Deaton, C. M., Poole, D. C., Kindig, C. A., Mcdonough, P. and Erickson, H. H. (2002). Movements of thoracic and abdominal compartments during ventilation at rest and during exercise. *Equine Vet. J. Suppl.* **34**, 384-390. doi:10.1111/j.2042-3306.2002.tb05453.x

McGuigan, M. P. and Wilson, A. M. (2003). The effect of gait and digital flexor muscle activation on limb compliance in the forelimb of the horse *Equus caballus*. *J. Exp. Biol.* **206**, 1325-1336. doi:10.1242/jeb.00254

O'Neill, M. C., Umberger, B. R., Holowka, N. B., Larson, S. G. and Reiser, P. J. (2017). Chimpanzee super strength and human skeletal muscle evolution. *Proc. Natl. Acad. Sci. USA* **114**, 7343-7348. doi:10.1073/pnas.1619071114

Pontzer, H. (2017). Economy and endurance in human evolution. *Curr. Biol.* **27**, R613-R621. doi:10.1016/j.cub.2017.05.031

Poole, D. C. and Erickson, H. H. (2011). Highly athletic terrestrial mammals: horses and dogs. *Comprehens. Physiol.* **1**, 1-37. doi:10.1002/cphy.c091001

Preuschoft, H. (2004). Mechanisms for the acquisition of habitual bipedality: are there biomechanical reasons for the acquisition of upright bipedal posture? *J. Anat.* **204**, 363-384. doi:10.1111/j.0021-8782.2004.00303.x

Saumarez, R. C. (1986). An analysis of possible movements of the human upper rib cage. *J. Appl. Physiol.* **60**, 678-689. doi:10.1152/jappl.1986.60.2.678

Sawilowsky, S. (2009). New effect size rules of thumb. *J. Mod. Appl. Stat. Methods* **8**, 467-474. doi:10.22237/jmasm/1257035100

Sawyer, G. J. and Maley, B. (2005). Neandertal reconstructed. *Anat. Rec.* **283B**, 23-31. doi:10.1002/ar.b.20057

Schmid, P. (1983). Eine Rekonstruktion des Skelettes von A.L. 288-1 (Hadar) und deren Konsequenzen. *Folia Primatologia* **40**, 283-306. doi:10.1159/000156111

Schmid, P., Churchill, S. E., Nalla, S., Weissen, E., Carlson, K. J., de Ruiter, D. J. and Berger, L. R. (2013). Mosaic Morphology in the Thorax of *Australopithecus sediba*. *Science* **340**, 109-236. doi:10.1126/science.1234598

Seeherman, H. J., Taylor, C. R., Maloiy, G. M. O. and Armstrong, R. B. (1981). Design of the mammalian respiratory system. II. Measuring maximum aerobic capacity. *Respir. Physiol.* **44**, 11-23. doi:10.1016/0034-5687(81)90074-8

Smith, C. A., Mitchell, G. S., Jameson, L. C., Musch, T. I. and Dempsey, J. A. (1983). Ventilatory response of goats to treadmill exercise: grade effects. *Respir. Physiol.* **54**, 331-341. doi:10.1016/0034-5687(83)90076-2

Szlyk, P. C., McDonald, B. W., Pendergast, D. R. and Krasney, J. A. (1981). Control of ventilation during graded exercise in the dog. *Respir. Physiol.* **46**, 345-365. doi:10.1016/0034-5687(81)90131-6

Taylor, R., Maloiy, G. M., Weibel, E. R., Langman, V. A., Kanmau, J. M., Seeherman, H. J. and Heglund, N. C. (1980). Design of the mammalian respiratory system III. scaling maximum aerobic capacity to body mass in wild and domestic animals. *Respir. Physiol.* **44**, 25-37. doi:10.1016/0034-5687(81)90075-X

Thorpe, C. T., Marlin, D. J., Franklin, S. H. and Colborne, G. R. (2009). Transverse and dorso-ventral changes in thoracic dimension during equine locomotion. *Vet. J.* **179**, 370-377. doi:10.1016/j.tvjl.2007.10.014

Tickle, P. G., Ennos, A. R. Lennox, L. E., Perry, S. F. and Codd, J. R. (2007). Functional significance of the unicinate process in birds. *J. Exp. Biol.* **210**, 3955-3961. doi:10.1242/jeb.008953

Trinkaus, E. (1983). *The Shanidar Neanderthals*. New York: Academic Press.

Weibel, E. R. (1984). *The Pathway for Oxygen*. Cambridge, MA: Harvard University Press.

Williams, S. A., García-Martínez, D., Bastir, M., Meyer, M. R., Nalla, S., Hawks, J., Schmid, P., Churchill, S. E. and Berger, L. R. (2017). The vertebrae and ribs of *Homo naledi*. *J. Hum. Evol.* **104**, 136-154. doi:10.1016/j.jhevol.2016.11.003

Wilson, T. A., Rehder, K., Krayer, S., Hoffman, E. A., Whitney, C. G. and Rodarte, J. R. (1987). Geometry and respiratory displacement of human ribs. *J. Appl. Physiol.* **62**, 1872-1877. doi:10.1152/jappl.1987.62.5.1872